Supporting Information

First-principles Design of a Borocarbonitride based Anode for Superior Performance in Sodium-ion Battery and Capacitor

Swastika Banerjee[a], Siamkhanthang Neihsial[b] and Swapan K. Pati[*ab]

[a]New Chemistry Unit, [b]Theoretical Sciences Unit,

Jawaharlal Nehru Centre for Advanced Scientific Research, Jakkur P.O., Bangalore 560064, India

Computational details:

ab initio Molecular Dynamics simulations (NVT; 300 K) are based on quantum density functional theory using the same protocol as used for structural optimisation in VASP. [1-3] The length and time scales achieved in this study are 20 ps and 1 fs, respectively. Nosé-Hoover [4-6] type thermostat has been applied as temperature bath.

We optimise the crystal geometry of $LiBH_4$ until the maximum residual atomic force becomes less than 1×10^{-3} Ry/bohr. The cut-off energies are 40 Ry and 320 Ry for the pseudowave functions and the charge density, respectively. 6×10×6 *k*-mesh has been used. We have checked that, these conditions give good convergence for the total energy within 1×10^{-4} Ry/atom. The obtained lattice constants are *a*=7.32Å, *b*=4.35Å, and *c*=6.62 Å with the deviation from the experimental values[1] are almost 2, −1, and −3%, respectively.

Since the unit cell contains four formula units with 24 atoms, there are 72 Γ-phonon modes, with 69 optical modes. The Gaussian broadening with a width of 25 cm^{-1} has been used. There are three separate regions of phonon frequencies, namely, region I: less than 500cm^{-1}, region II: 1000 to 1300cm^{-1}, and region III: 2250 to 2400cm^{-1} (see Fig. S13 in S.I.). Lower frequency region (region I) is mainly contributed by the Li displacements. On the other hand, internal B-H bending and stretching vibrations of BH_4 complexes give rise to the regions II and III, respectively implying strong internal bonding of BH_4 complexes. These finding corroborates well with previous findings as shown in ref. 39.

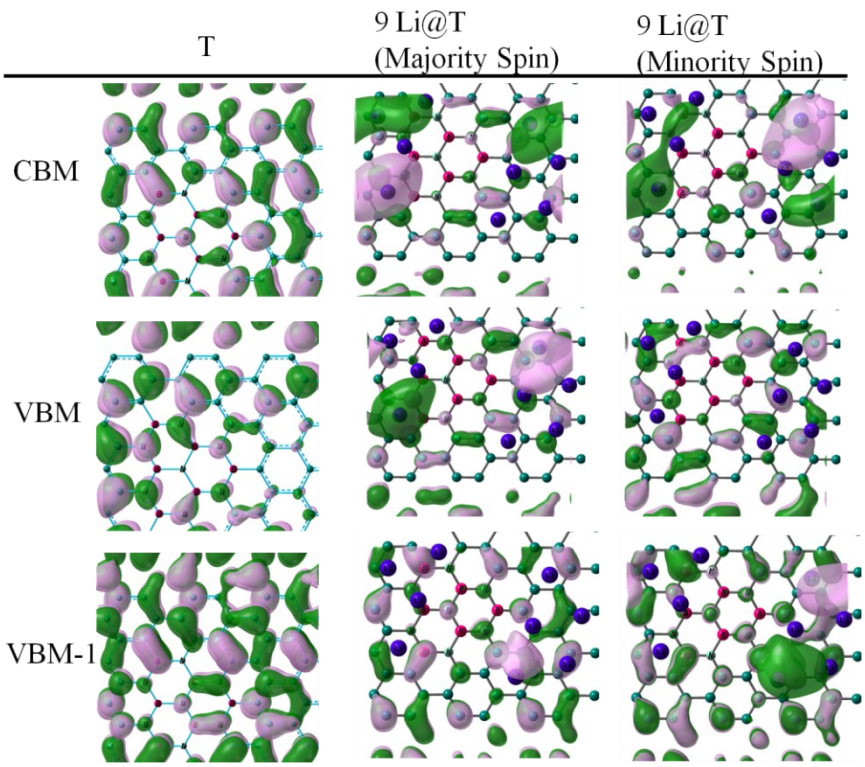

Figure S1. Real space wave function plot corresponding to the valence band maxima (VBM), VBM-1 and conduction band minima (CBM) states for fully charged state while T_N has been considered as the anode. Strong bonding in Li cluster is evident from prevalence of electron density. Iso value used for these plots is 0.02 and density 0.05 e $Bohr^{-3}$.

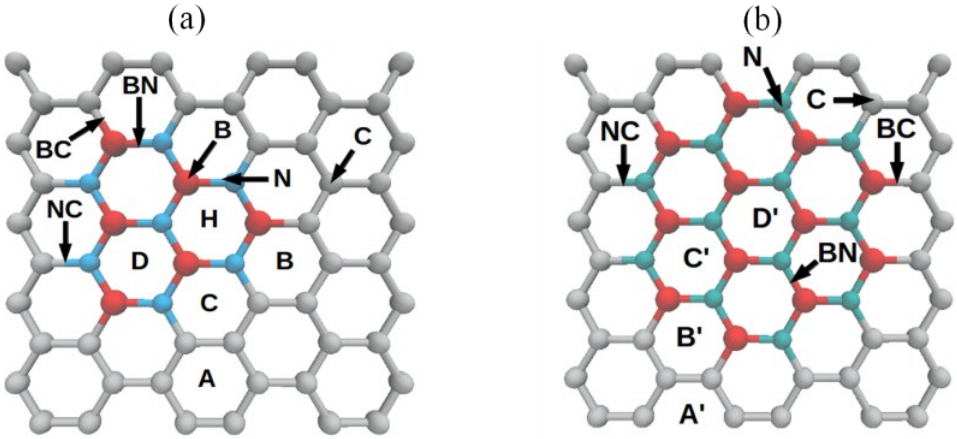

Figure S2. For ‘m’ type, there are four possible adsorption sites, which are denoted as A, B, C and D (A′, B′, C′ and D′). Relative energy differences for Li-adsorption process on these sites have been given for low Li-concentration (x = 0.02) Table 3. Other sites shown by the arrows are ‘t’site.

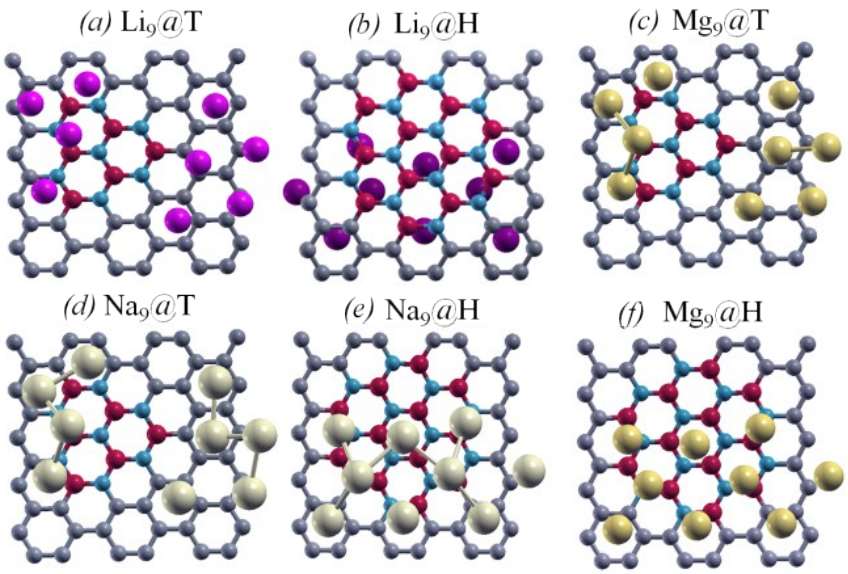

Figure S3. Optimized stable configurations of 9 atoms (Li, Na and Mg) adsorbed on the monolayer BCN.

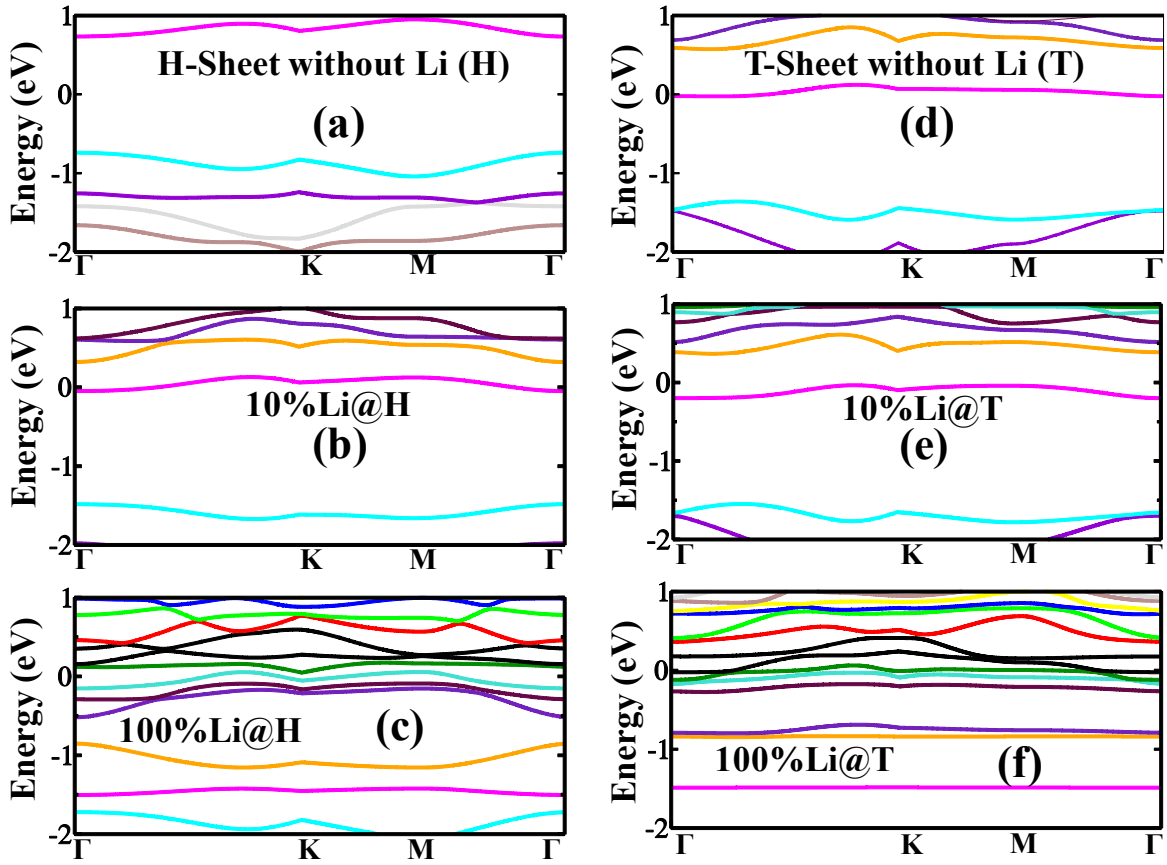

Figure S4. Band dispersion of (a) 'T', (b) 'H' sheets, at different concentration of adsorbed Li. Γ = (0, 0, 0), *K* = (0, 0.5, 0), *M* = (0.5, 0.5, 0).

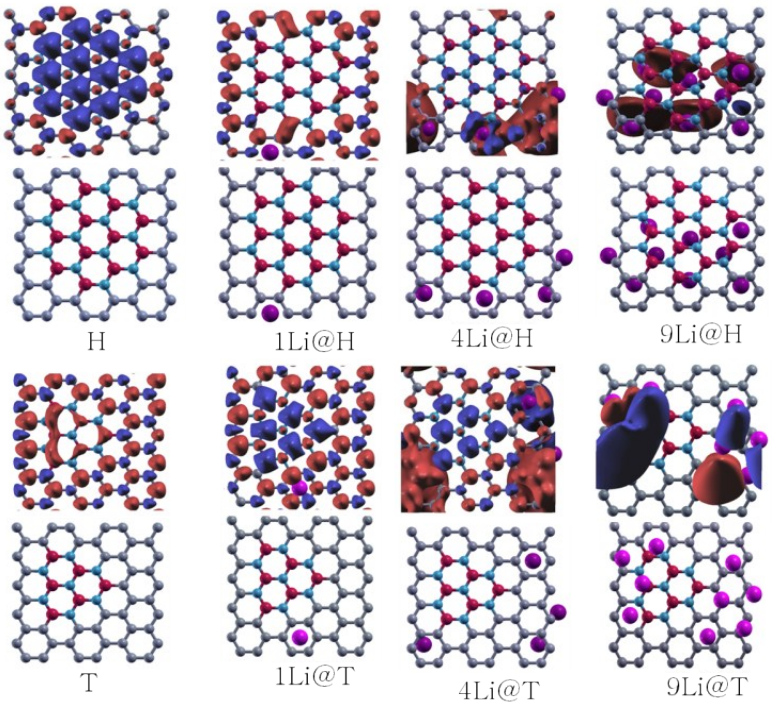

Figure S5. Optimized stable configurations of n Li atoms adsorbed on the monolayer BCN: (a) n = 0, (b) n = 1, (c) n = 4, (d) n = 9. Charge density with an isosurface value of 0.01e/Å^3 for borocarbonitride monolayer and the same with Li adsorbed at different concentration. The red and blue regions indicate an increase and decrease in electron density, respectively.

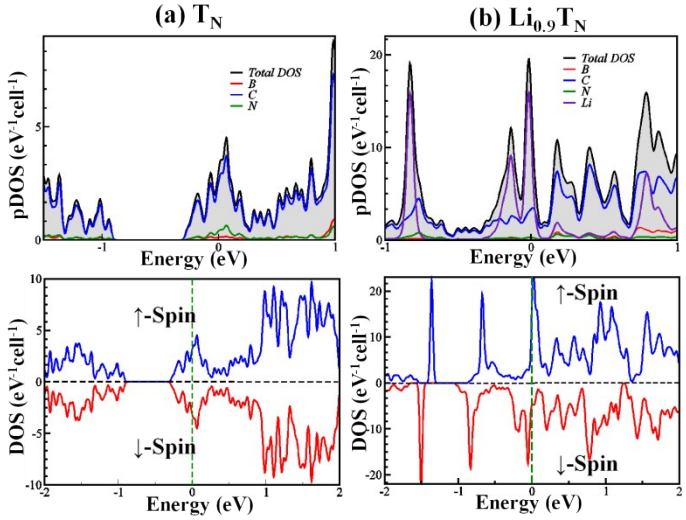

Figure S6. Total density of states (DOS) and projected density of states (PDOS) for pristine T_N-sheet as well as its lithiated state in (a) and (b) respectively.

Trigonal BN nano-domains embedded on graphene results in metallic (non-spin-polarized) ground states but after lithiation it remains metallic with additional spin-polarization with full control over its spin components which can find application in spintronic devices.

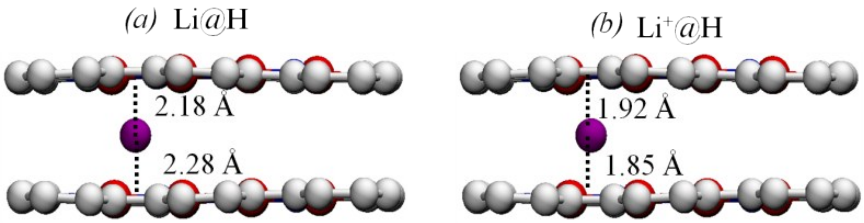

Figure S7. (a) Optimized stable configurations (side view) of lithium atom intercalated bilayer H sheet. (b) Optimized stable configurations (side view) of lithium ion intercalated bilayer H sheet.

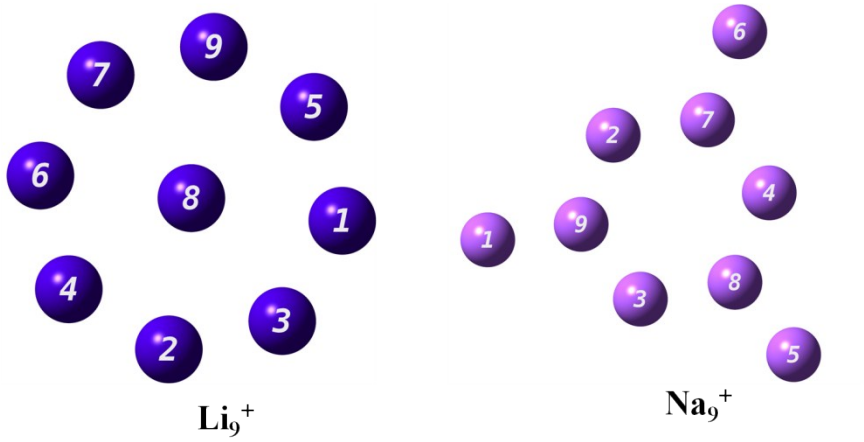

Figure S8. Stable configurations (2D view) of lithium and sodium cluster (positively charged).

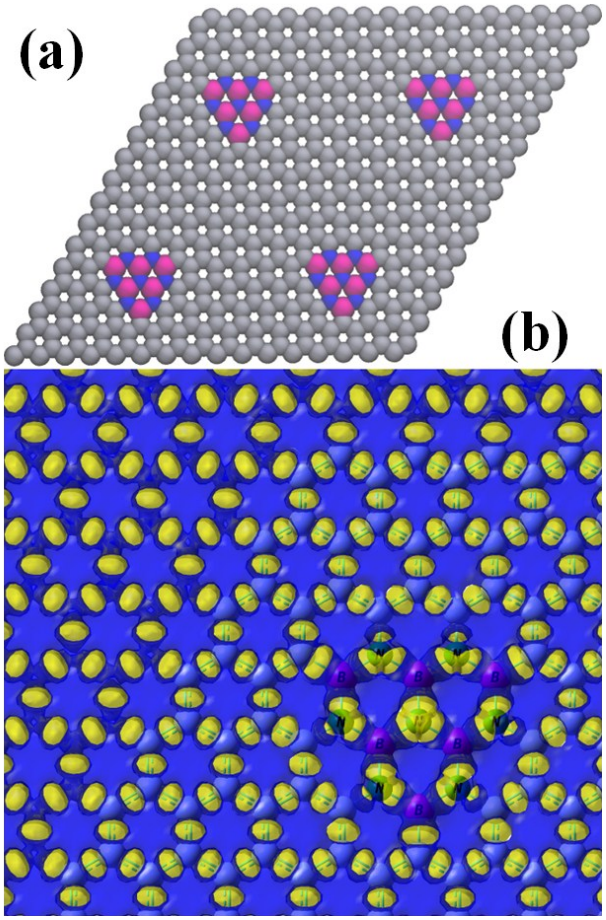

Figure S9. (a) Monolayer $B_xC_yN_z$: x = 6, y = 115 and z = 7, with overall 10% BN concentration with trigonal BN-domain. (b) Differential Charge density plot is shown with an iso-surface value of 0.02 and density of 0.01e/Å^3. The yellow and blue regions indicate an increase and decrease in electron density, respectively.

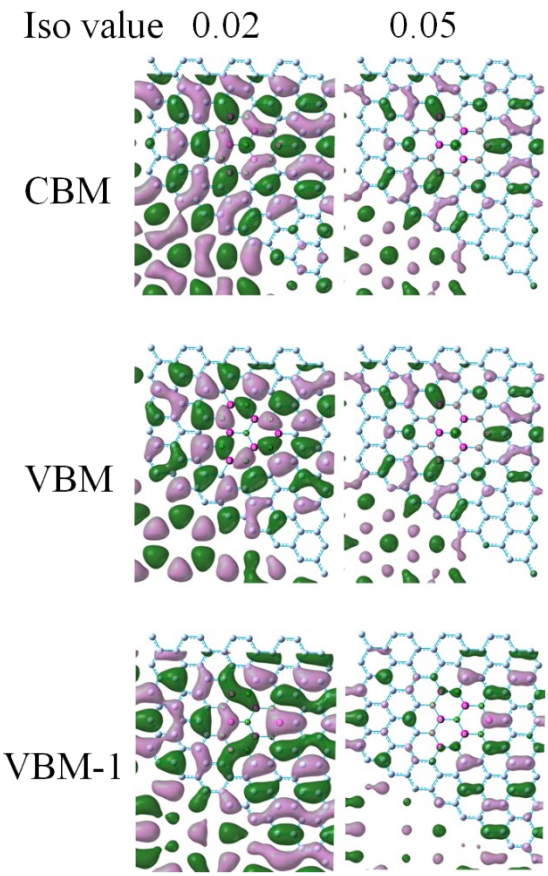

Figure S10. Real space wave function plot corresponding to the valence band maxima (VBM), VBM-1 and conduction band minima (CBM) states for borocarbonitride-monolayer with 10% BN concentration (with trigonal BN-domain). Two different iso-density plots have been shown. Iso value used for these plots is 0.02 and values of the density are 0.02 and 0.05 e Bohr^{-3}, respectively from left to right column.

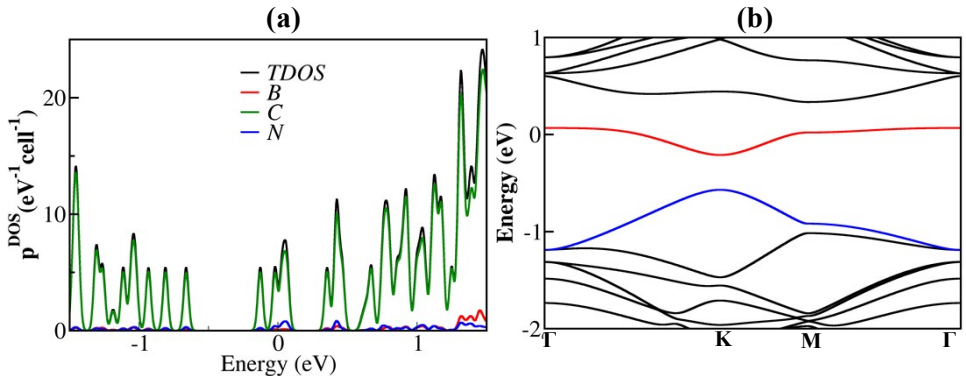

Figure S11. (a) Total density of states (TDOS) and projected density of states (P^{DOS}) for BCN-sheet with 10% BN concentration (with trigonal BN-domain). Fermi energy

(E_F) has been rescaled at zero. (b) Band dispersion pattern (path: Γ-X-M-Γ) is shown. Γ = (0, 0, 0), *K* = (0, 0.5, 0), *M* = (0.5, 0.5, 0).

The system of our interest is 2D and the floppy mode of vibration for such sheet is generally negligibly small and thus not considered usually in the literature. At the charged state, ions (Li, Na) get adsorbed on the surface via a strong chemisorption with a wide range of binding energy (1.00-2.50 eV/atom), depending on the type of ad-atom and the binding-site. Such strong bonding of the ad-atom with the matrix results in the decrease in conformational flexibility. So, the configurational entropy term at both the charged and discharged state can be assumed to be negligibly small. However, to have a quantitative estimation of the TS (G = H -TS), we have carried out an additional calculations based on ab-initio molecular dynamics at 300 K. We find that, the structural vibration leads to TS value of 0.00025 eV/atom for T_N sheet as anode at completely discharged state which reaches the value of 0.00045 eV/atom at fully charged state(see Figure S12). Thus, TS is negligibly small compared to the OCV (~1.25 eV for Sodium ion battery and >1.50 for Lithium ion battery), computed through consideration of purely electronic degrees of freedom.

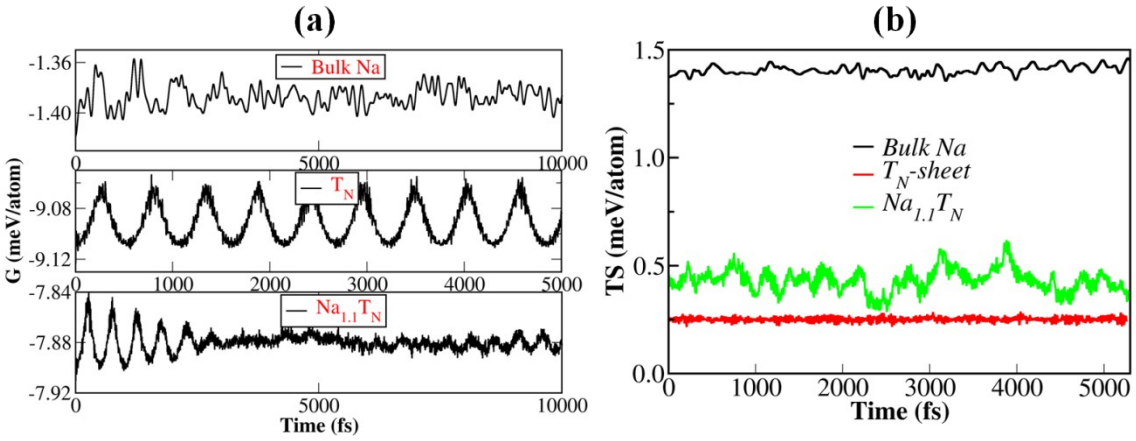

Figure S12. Results on the basis of free energy calculation as derived from the AIMD study. (a) Free Energy and (b) the energy term originated from entropy in thermally equilibrated T_N system at 300K. The fully charged state ($Na_{1.1}T_N$), pure sheet (T_N) and bulk Na have been compared.

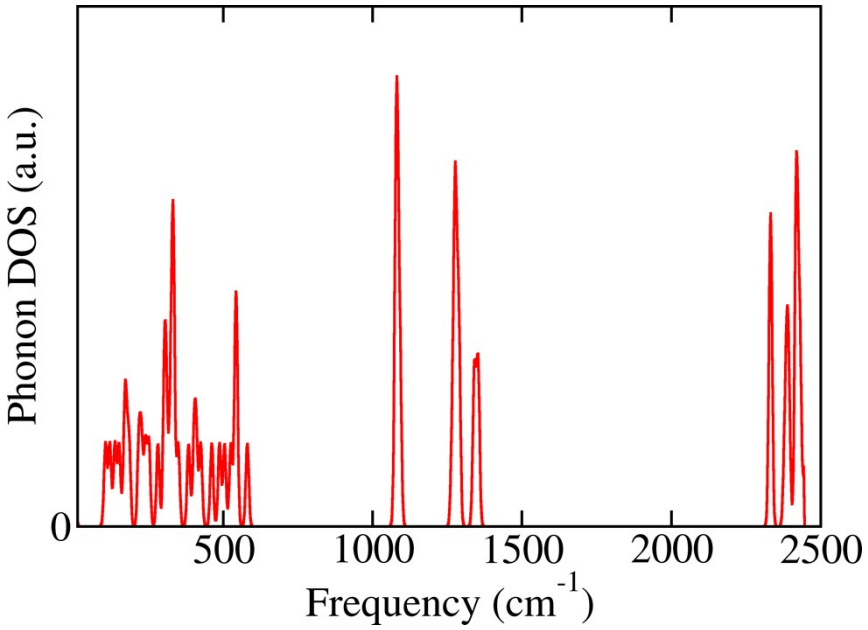

Figure S13. Phonon density of states for orthorhombic $LiBH_4$. The contribution of the optical Gamma-phonon modes is taken into account. Gaussian broadening with a width of 25 cm^{-1} has been used.

Table S1. Bader charge (e) on the Lithium and Sodium atoms in the Li and Na clusters as shown in Figure S8). Atom numbers are shown in Figure S8.

Atom No.	Li	Na
1	0.01	-1.03
2	0.02	+0.98
3	0.02	+0.98
4	0.05	+0.98
5	-0.02	-1.03
6	-0.02	-1.03
7	+0.04	+0.98
8	+0.98	+0.98
9	-0.03	-0.74

1. G. Kresse and J. r. FurthmÃ¼ller, *Computational Materials Science*, 1996, **6**, 15-50.
2. G. Kresse and J. r. FurthmÃ¼ller, *Physical Review B*, 1996, **54**, 11169.
3. D. Marx and J. Hutter, *Modern methods and algorithms of quantum chemistry*, 2000, **1**, 301-449.
4. S. NosÃ©, *The Journal of chemical physics*, 1984, **81**, 511-519.
5. W. G. Hoover, *Physical Review A*, 1985, **31**, 1695.
6. G. J. Martyna, M. L. Klein and M. Tuckerman, *The Journal of chemical physics*, 1992, **97**, 2635-2643.